

Article

Dewatering Characteristics and Drawdown Prediction of Suspended Waterproof Curtain Foundation Pit in Soft Soil Areas

Yuhan Chu ^{1,*}, Junfeng Shi ¹, Zhaoyi Ye ²  and Dingdan Liu ¹

¹ School of Civil Engineering, Architecture and Environment, Hubei University of Technology, Wuhan 430068, China; 19981034@hbut.edu.cn (J.S.); 102111013@hbut.edu.cn (D.L.)

² School of Computer Science, Hubei University of Technology, Wuhan 430068, China; 102101051@hbut.edu.cn

* Correspondence: 102110864@hbut.edu.cn (Y.C); Tel.: +86-18137110651

Abstract: Suspended waterproof curtains combined with pumping wells are the primary method for controlling groundwater levels in foundation pits within soft soil areas. However, there is still a lack of a systematic approach to predict the groundwater drawdown within the foundation pit caused by the influence of these suspended curtains. In order to investigate the variation of groundwater level within the excavation during dewatering processes, the finite difference method is employed to analyze the seepage characteristics of foundation pits with suspended waterproof curtains. Basing on the concept of equivalent well, this study examines the coupled effects of aquifer anisotropy (k_i), aquifer thickness (M_i), well screen length (l_i), and the depth of waterproof curtain embedment on the seepage field distortion. A characteristic curve is established for standard conditions, which exposes the blocking effect of the curtain on the amount of groundwater drawdown in the pit. Additionally, correction coefficients are proposed for non-standard conditions, which, in turn, results in a prediction formula with a wider range of applicability. Comparative analysis between the calculated predictions and the field observation data from an actual foundation pit project in Zhuhai City validates the feasibility of the quantitative prediction method proposed in this research, which also provides a 21% safety margin.

Keywords: phreatic aquifer; the Pearl River Delta; groundwater seepage; barrier; drawdown; dewatering



Citation: Chu, Y.; Shi, J.; Ye, Z.; Liu, D. Dewatering Characteristics and Drawdown Prediction of Suspended Waterproof Curtain Foundation Pit in Soft Soil Areas. *Buildings* **2024**, *14*, 119. <https://doi.org/10.3390/buildings14010119>

Academic Editor: Dong Su

Received: 7 November 2023

Revised: 14 December 2023

Accepted: 30 December 2023

Published: 2 January 2024



Copyright: © 2024 by the authors. Licensee MDPI, Basel, Switzerland. This article is an open access article distributed under the terms and conditions of the Creative Commons Attribution (CC BY) license (<https://creativecommons.org/licenses/by/4.0/>).

1. Introduction

As urbanization accelerates in southern coastal regions of China, the population density continues to rise, leading to an increasing demand for the construction of large buildings along the coastal areas [1]. Foundation pits, as primary underground structures for constructing large buildings, have seen a continuous increase in both quantity and depth, along with an expanding excavation area. In coastal regions of the Pearl River Delta, China (e.g., Zhuhai, Zhongshan, and Jiangmen), with abundant groundwater in aquifers [2], the risks associated with dewatering during construction have correspondingly grown [3–5]. To ensure a safe construction environment within the foundation pit, the application of dewatering measures in excavation projects has also extended to a broader scope [6]. In contrast to inland areas, the soil in coastal regions is primarily composed of alluvial convergent sediments by rivers and marine soft sediments alternately, mainly consisting of silt sand and low-permeability clay. These soil layers are characterized by high compressibility and low permeability [7,8]. Due to the large thickness of the submerged layer, the majority of groundwater aquifers are categorized as phreatic aquifers rather than confined aquifers. In addition, the initial groundwater tables are generally higher in coastal areas, and most of the target depths of excavation for many building foundation pit projects are lower than the location of the initial groundwater tables [9], which is more significantly affected by the groundwater level.

The excavation process in these areas does not isolate the hydraulic connection between the inside and outside of the foundation pit, resulting in a difference in the hydraulic head, which allows groundwater to flow into the pit [10]. To prevent issues such as sand inflow, sudden floor heave, and water inflowing towards the excavation [11,12], it is crucial to implement necessary dewatering measures. Additionally, improper dewatering can lead to rapid ground settlement, potentially causing damage to nearby structures, especially in densely populated urban areas [13,14]. In preventing major financial and material losses resulting from dewatering accidents, it is of utmost importance to prudently control the groundwater level within the foundation pit, ensuring the safety and stability of the construction site, which holds significant practical significance. Dewatering of excavation aims to minimize surrounding ground settlement and pumping volume while ensuring a safe and dry construction environment and avoiding the waste of water resources. The common approach to controlling groundwater pressure involves the use of low-permeability materials such as cement mixing piles, jet-grouted piles, and diaphragm walls [15–17] as waterproof curtains, combined with pumping wells for dewatering. Curtain as a waterproof structure of the pit project can effectively reduce the hydraulic connection between the inside and outside of the pit, block the seepage of groundwater in the direction of the pit [18–20], and also play the role of supporting structure. Waterproof curtains can be categorized as penetrating curtains and suspended waterproof curtains based on whether they fully penetrate aquifers. In theory, penetrating waterproof curtains can entirely block hydraulic connections between the inside and outside of the excavation. However, they often encounter challenges when attempting to penetrate aquifers, leading to potential defects [21]. Thick aquifer layers not only limit the practicality of fully penetrating curtains but also make the exposed curtain above the pit bottom vulnerable to localized cracking and leakage due to the external soil pressure after excavation, posing a risk to construction safety [22]. Consequently, suspended waterproof curtains are becoming increasingly popular in foundation pit dewatering projects when compared to full penetrating waterproof curtains.

To investigate the blocking effect induced by suspended waterproof curtains [23], numerical simulation methods such as MODFLOW finite difference software [24–26] have been widely adopted by many researchers. Studies have shown that the hydraulic isolation provided by the curtain is manifested in three key aspects: extending the groundwater seepage path, altering the seepage direction, and reducing the seepage area [27]. Furthermore, the permeability anisotropy and the thickness of the aquifer [28,29] also have certain impacts on groundwater seepage. Presently, the construction methods for waterproof curtains have become increasingly mature, while the coupled blocking effect of pumping wells and curtains has been studied at a deeper level [30,31]. A large number of experiments have been used to verify the dewatering effect of wall–well coupling. The application of numerical simulation methods aids in determining the optimal embedment depth of the curtain [32] and evaluating the feasibility of dewatering methods [33], which provides a reference for the study of the seepage mechanisms and field application of suspended waterproof curtains. Research into the inflow prediction and head differences on both sides of the waterproof curtain for confined aquifer excavation has been extensive [34,35]. However, methods for forecasting drawdown in the foundation pit after the operation of dewatering wells often rely heavily on numerical simulations. Such research approaches are hindered by their high modeling complexity, intensive computational requirements, and limited range of applicability. Many of these studies primarily consider the embedding depth of waterproof curtains as a single variable and explore its impact on groundwater seepage without considering the coupled effects of various influencing factors. To make up for the lack of research on groundwater seepage characteristics during the dewatering process of foundation pits in phreatic aquifers, this study aims to quantitatively assess the blocking effects of curtains, taking into account the anisotropy of permeability, aquifer thickness, and the length of the well screen in dewatering wells, to derive a more widely applicable formula for predicting drawdown in unconfined aquifer foundation pits and provide a

reference method for the prediction of the effectiveness of the design and construction monitoring of similar foundation pits dewatering in the soft soil areas. To address the problem, this paper first analyzes the seepage mechanisms of suspended waterproof curtains in unconfined aquifers. Subsequently, numerical simulation software MODFLOW is employed to solve standard and variational functions that influence groundwater seepage. Finally, a comparative analysis between the numerical solutions and field observations is conducted to validate the applicability of the proposed equations.

2. Seepage Mechanisms under the Influence of Waterproof Curtain

2.1. Seepage Analysis

When conducting dewatering operations within an unconfined aquifer foundation pit, groundwater from the surrounding aquifer flows into the dewatering well, resulting in a lowering of groundwater levels in the central region of the well and its immediate vicinity. The influence of the dewatering well on drawdown in the surrounding aquifer becomes less pronounced as the distance from the well center increases. The maximum drawdown occurs at the well center and decreases as the well diameter moves outward from the center of the well. The overall drawdown profile exhibits a continuous funnel-like shape, as illustrated in Figure 1a.

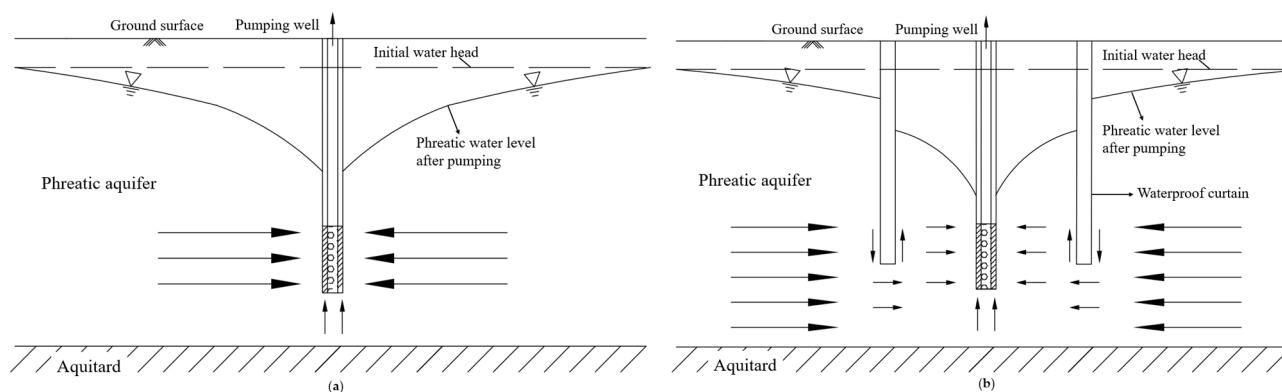


Figure 1. Profile view of groundwater seepage and partial pumping well in phreatic aquifer. (a) Without curtain. (b) With curtain.

Since dewatering wells do not fully penetrate the aquifer to the aquitard, groundwater near the dewatering well bottom experiences a complex three-dimensional (3D) seepage field. To simplify the description of groundwater seepage, horizontal and vertical seepage are used as substitutes for 3D seepage. After the installation of the waterproof curtain, the seepage environment around the foundation pit site is influenced, resulting in changes to the groundwater flow field near the curtain. The hydraulic containment effects of the curtain are primarily manifested in three aspects [36,37]:

1. Alteration of seepage direction and elongation of the seepage path: In the absence of the waterproof curtain, groundwater flows horizontally into the well along the radial direction of the pumping well, with vertical seepage occurring around the pumping well, as shown in Figure 1a. However, with the installation of the waterproof curtain during dewatering, there is a change in the direction of groundwater flow outside the curtain at the base of the curtain, as depicted in Figure 1b. Groundwater outside the foundation pit site needs to circumvent the bottom of the waterproof curtain to reach the vicinity of the pumping well, resulting in an extended flow path compared to when no curtains are in place.
2. Modification of groundwater drawdown within and outside the foundation pit: In the absence of the curtain, the drawdown profile exhibits a continuous funnel shape. However, when the waterproof curtain is installed, water levels inside and outside

the excavation show a head difference on either side of the curtain, leading to a discontinuous, step-like drawdown profile on both sides of the curtain.

- Reduction in the total inflow to the foundation pit: According to Darcy's law [38], when pumping is conducted at a constant flow rate, the elongation of the groundwater flow path due to the presence of the waterproof curtain leads to a reduced seepage area. This decrease in seepage area results in an increased hydraulic gradient, reducing the required dewatering time and improving dewatering efficiency. Consequently, this leads to a reduction in the overall seepage volume within the foundation pit.

All of the above descriptions of groundwater seepage movement patterns in phreatic aquifers are based on the following assumptions:

- The groundwater flow towards the well is assumed to be approximately horizontal.
- The aquifer is considered to be homogeneous, isotropic, of uniform thickness, and laterally infinite.
- Before pumping, the natural hydraulic gradient in the aquifer is assumed to be zero.
- Pumping is assumed to be of long duration, and groundwater flow within the aquifer is expected to follow Darcy's law, reaching a state of steady flow.

2.2. Drawdown in Equivalent Well

As illustrated in Figure 2a, based on the Dupuit theory of drawdown curves [39], the foundation pit with the suspended waterproof curtain can be analogously represented as a two-dimensional partial pumping well of radius r_0 (the radius of the equivalent pumping well for the excavation) in the phreatic aquifer. The calculation of the drawdown in the equivalent well using the Theis formula [40] can be expressed as follows:

$$s_t = s - \frac{s^2}{2H} = \frac{Q_w}{4\pi T} \ln \frac{2.25Tt}{r_0^2 S} \quad (1)$$

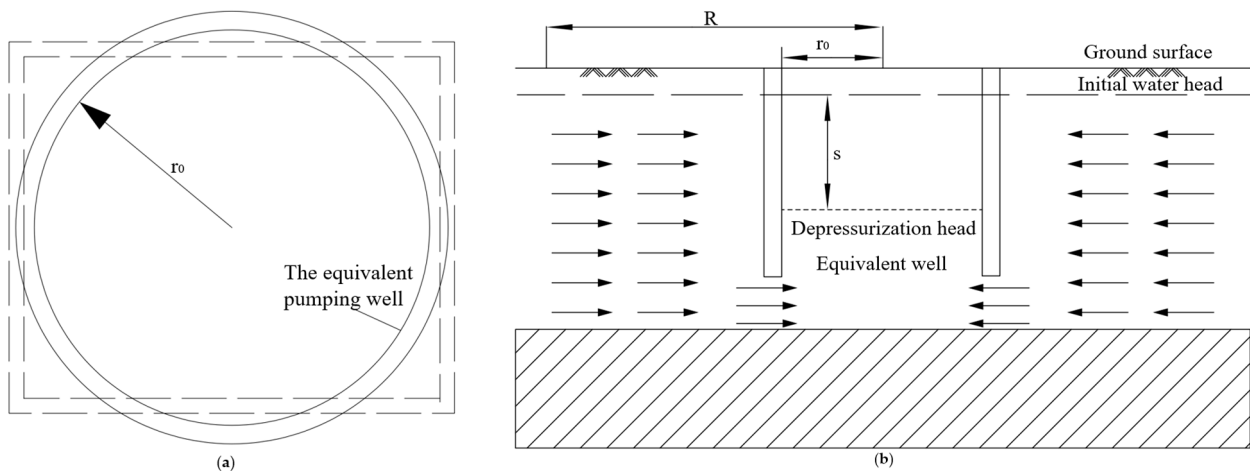


Figure 2. Equivalent pit precipitation well. (a) Top view of equivalent well. (b) Profile view of equivalent well.

In the equation, the variables are defined as follows: s_t represents the drawdown in water level at the location r_0 (m); Q_w stands for the flow rate of the equivalent dewatering well associated with the excavation (m^3/d); T is transmissivity of the aquifer (m^2/d), where $T = KH$ (K : hydraulic conductivity; H : aquifer thickness); S denotes the specific storage coefficient of the aquifer indicates the characteristics of the water outflow when the water level within the aquifer decreases; s corresponds to the observed drawdown in water level (m); r_0 is the radius of the equivalent pumping well for the excavation, calculated as $r_0 = \sqrt{\frac{A}{\pi}}$, where A represents the area of the excavation (m^2); and H signifies the thickness of the phreatic aquifer (m).

According to the Theis equation, it is evident that the transmissivity (T) and the thickness of the phreatic aquifer (H) directly influence the drawdown in water level after dewatering of the equivalent well associated with the foundation pit. However, this calculation method does not take into account the indirect effects caused by the distortion of the seepage field. The blocking effect of the waterproof curtain induces a complex three-dimensional flow rather than a parallel flow, leading to changes in seepage direction, paths, and seepage area, which subsequently deform the seepage field. Hence, the blocking effect of the waterproof curtain cannot be overlooked and requires the introduction of quantifying coefficients.

3. Numerical Simulation

For the equivalent circular foundation pit described above, a numerical model is established based on typical geological properties in the soft soil areas of the Pearl River Delta, China [41]. The foundation pit radius, denoted as r_0 , is set at 53 m, with a waterproof curtain thickness of 1 m. To stabilize the seepage flow in the model, based on the empirical dewatering scheme, the total dewatering time is set to be 100 days. The groundwater flow in the numerical model is approaching a steady state in this state.

3.1. Governing Equation

In order to obtain a conservative estimate for the drawdown design values, the assumptions of Darcy law and continuity are employed, neglecting no-Darcy flow. Considering the effect of unsteady flow, modeled groundwater 3D unsteady flow in the study area is controlled by the following equation. The formulation includes the establishment of a groundwater flow governing equation, initial groundwater head, and boundary conditions within a saturated porous medium [38]:

$$\begin{aligned} \text{governing equation : } & \frac{\partial}{\partial x} \left(K_{xx} \frac{\partial h}{\partial x} \right) + \frac{\partial}{\partial y} \left(K_{yy} \frac{\partial h}{\partial y} \right) + \frac{\partial}{\partial z} \left(K_{zz} \frac{\partial h}{\partial z} \right) - Q = S_s \frac{\partial h}{\partial t} \\ \text{initial groundwater head : } & h(x, y, z) \Big|_{t=t_0} = h_0(x, y, z, t) \quad (x, y, z) \in \Gamma_1 \\ \text{boundary conditions : } & K_{xx} \frac{\partial h}{\partial n_x} + K_{yy} \frac{\partial h}{\partial n_y} + K_{zz} \frac{\partial h}{\partial n_z} \Big|_{\Gamma_2} = q(x, y, z, t) \\ & h(x, y, z) \Big|_{\Gamma_1} = h_1(x, y, z, t) \end{aligned} \quad (2)$$

In the equation, K_{xx} , K_{yy} , and K_{zz} represent the hydraulic conductivities in the x , y , and z directions, respectively (cm/s); h is the groundwater level at point (x, y, z) (m); Q is the groundwater recharge and discharge (d^{-1}); S_s represents the specific storage at point (x, y, z) (m^{-1}); T is the elapsed time (h); h_0 is the initial groundwater level at point (x, y, z) (m); Γ_1 and Γ_2 correspond to the first and second class boundary conditions, respectively; n_x , n_y , and n_z are the unit normal vectors along the x , y , and z directions for boundary Γ_2 ; and q is the lateral inflow per unit area on boundary Γ_2 (m^3/d). In this simulation, it is assumed that the soil is isotropic in the horizontal direction, meaning K_{xx} equals K_{yy} .

3.2. Finite Difference Model

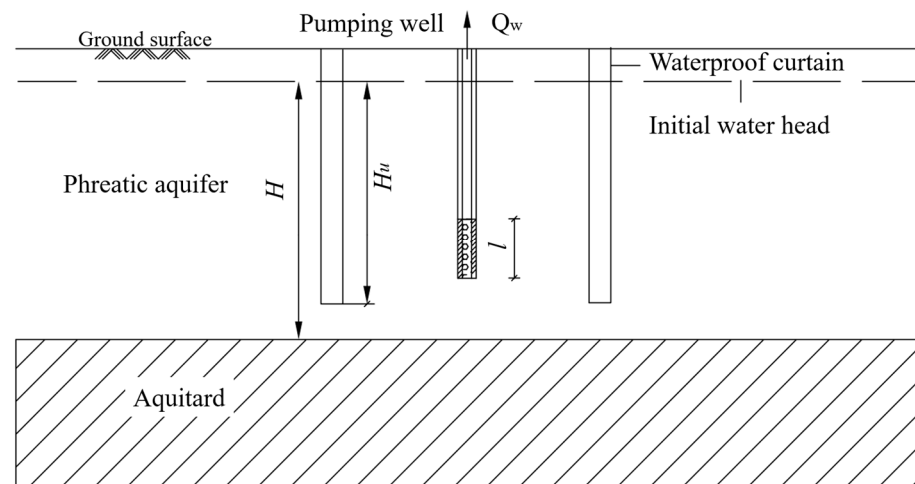
3.2.1. Simplification of Model Parameters

Table 1 outlines the parameters of the simplified calculation model. A phreatic aquifer (which allows the movement of water through it under ordinary conditions) and an aquitard (which has poor permeability and hence will not yield water freely to wells) are considered at 60 m depth. The soil types of the phreatic aquifer are backfill and sandy clay. The soil type of aquitard is silty clay. In the numerical simulation calculations, it is assumed that the soil is isotropic.

Table 1. Simplification of model parameters.

Soil Layer	H/m	$K_h/(m \cdot d^{-1})$	$K_v/(m \cdot d^{-1})$	$S_s/(10^{-3}m^{-1})$	e
Backfill	4	0.5	0.5	-	0.49
Sandy clay	36	2	2	2	0.43
Silty clay	20	0.001	0.001	5	0.56

To investigate the groundwater drawdown under the coupled influence of waterproof curtain and pumping wells, the analysis is conducted under standard conditions, with the waterproof curtain embedding depth (H_u) set at 36 m. The length of the well screen (l) is equal to H_u , the initial groundwater table in the phreatic aquifer is 2 m, and the aquifer thickness (H) is selected as 38 m, as depicted in Figure 3.

**Figure 3.** Profile view of curtain and aquifers.

3.2.2. Initial Boundary Conditions

To mitigate boundary effects, it is essential to determine appropriate model dimensions. Siechart's [42] empirical formula is employed to calculate the influence radius of the equivalent well of the phreatic aquifer foundation pit:

$$R = 2s\sqrt{HK} \quad (3)$$

In the equation, R represents the influence radius of the equivalent well (m); H is the aquifer thickness before pumping (m); K is the aquifer permeability coefficient; and s denotes the drawdown in the equivalent well.

In accordance with the requirements, considering an aquifer thickness of 38 m, the calculated drawdown influence radius is 259 m. Consequently, as illustrated in Figure 4a, the equivalent circular well radius (r_0) of the model is set to 54 m, and the finite difference model extended 260 m in all directions. This resulted in the creation of a three-dimensional grid with dimensions measuring 700 m in length and width, and 60 m extending in the z -axis direction. The model is divided into 42 layers, 4 for aquitard and 38 for phreatic aquifer, with 88 columns of values in 96 rows horizontally. The grid is fine in the excavation area of the pit. The grid is coarse at the edge of the excavation.

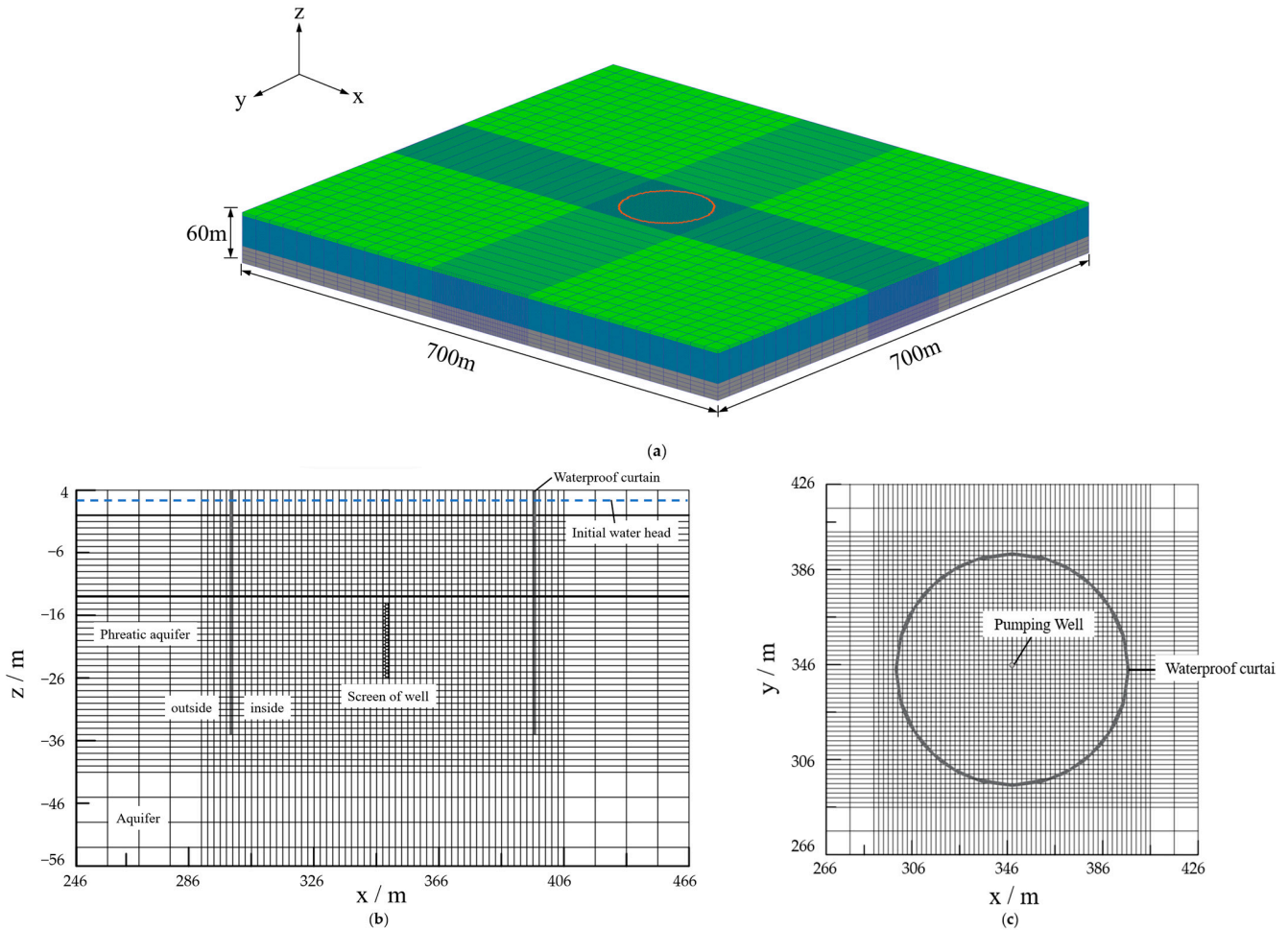


Figure 4. Finite difference mesh. (a) Three-dimensional. (b) Mesh in profile. (c) Mesh in plan.

The boundary conditions of the model are defined with constant head to simulate hydraulic recharge far from the source-sink terms [43], ensuring that the boundary remained at the original head level, unaffected by the drawdown within the foundation pit, as shown in Figure 4b. Referring to hydrogeological survey data, the initial groundwater level for the project is set at 2 m. Within the conceptual model of the excavation established by simulation, the pumping well and cutoff curtain units are projected onto the computational grid. At the well screen, a constant flow boundary condition is established to simulate drainage, while the waterproof curtain is represented by low-permeability units of 1×10^{-5} . To ensure conservative results, the model employed the parameters listed in Table 1. Figure 4c illustrates the positions of the pumping well and the waterproof curtain configuration.

3.3. Drawdown Coefficient

Adjust the pumping volume (Q_w) of the equivalent well in the three-dimensional numerical model to solve the groundwater drawdown s_c after pumping by the action of the waterproof curtain. The Theis theoretical solution (s_t) is linearly related to Q_w . The coefficient s_i of the influence of three-dimensional seepage caused by different depths of embedment of the waterproof curtain on the depth of the groundwater drawdown within a certain pumping flow rate can be expressed as follows:

$$s_i = s_c / s_t \quad (4)$$

3.4. Normalized Form

To ensure non-dimensional computational conditions, dimensionless form parameters are introduced, including the waterproof curtain embedment ratio ($b_i = H/H_u$), the permeability anisotropy ($k_i = k_h/k_v$), the thickness of phreatic aquifer ($H_i = H/38$), and the well screen length ($l_i = l/H_u$), serving as influencing parameters. For this study, the parameter values are set as $k_i = 1$, $H_i = 1$, and $l_i = 1$, representing the normalized situation for investigating the influence of the waterproof curtain on drawdown within the foundation pit. Under these standard conditions, different waterproof curtain embedment ratios, the Theis analytical solution curves (Q_w-s_t), and the numerical model results (Q_w-s_c) are presented in Figure 5a.

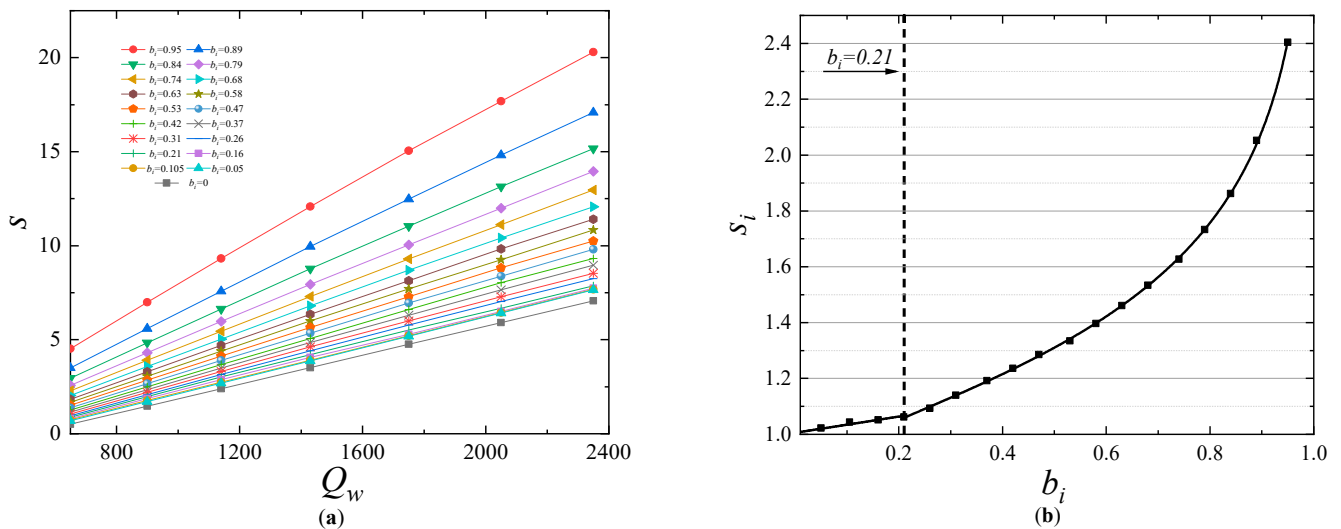


Figure 5. Variation results in the standard state. (a) Q_w-s curves with different b_i . (b) Normalized curve.

Figure 5 illustrates the impact of the cutoff barrier configuration on the distribution of the seepage field both within and outside the foundation pit. The presence of the cutoff barrier leads to an extension of groundwater flow paths outside the excavation, reducing the seepage area and causing a redistribution of hydraulic heads around the curtain. The simulation results indicate that horizontal groundwater flow predominantly occurs in the lower aquifer region beneath the waterproof curtain. The presence of the waterproof curtain necessitates the dissipation of a greater amount of vertical hydraulic potential energy in groundwater flow, leading to a weakening of the hydraulic connection between the interior and exterior of the foundation pit.

Under the influence of the waterproof curtain, groundwater seepage follows Darcy's law. As observed in Figure 5a, the Q_w-s curves exhibit linear distribution for different depths of cutoff wall insertion, indicating that with a constant pumping volume, greater waterproof curtain insertion depths result in a more significant drawdown within the foundation pit, signifying a more pronounced blocking effect on groundwater seepage. However, different waterproof curtain insertion ratios (b_i) lead to variations in the slopes of the Q_w-s curves. The impact of waterproof curtain insertion depth on the drawdown is quantified by the ratio of the slopes of Q_w-s_c and Q_w-s_t , representing the influence coefficient (s_i). The curve in Figure 5b illustrates that, under standard conditions, increasing the waterproof curtain insertion ratio intensifies the drawdown within the foundation pit. In other words, deeper cutoff walls enhance the blocking effect on groundwater seepage. As the depth of cutoff wall insertion increases, the slope of the Q_w-s curve continually rises. The b_i-s_i curve demonstrates that the blocking effect of the waterproof curtain grows linearly and then logarithmically with increasing b_i . When b_i approaches 1, it can be

considered that the cutoff walls entirely cut hydraulic connections between the interior and exterior of the foundation pit, resulting in the maximum s_i value.

In addition, there is a linear and nonlinear turning point in the fitted b_i - s_i curve, which is usually regarded as the blocking ratio in the case of an abrupt change in the groundwater drawdown discipline in the available numerical solutions and experimental studies of the model. In this study, $b_i = 0.21$ is selected as the break point and fits the b_i - s_i curve for the standard aquifer conditions. The fitting results are presented in Equation (5) (with correlation coefficients R_1^2 and R_2^2 of 0.958 and 0.999 for linear and exponential functions, respectively).

$$s_i = \begin{cases} 0.29b_i + 1.005 & b_i \leq 0.21 \\ 0.699 \ln(4.261b_i^{0.063} / (1 - b_i)^{0.669}) & b_i > 0.21 \end{cases} \quad (5)$$

4. Analysis of Factors Affecting Seepage

The numerical model established above is based on an assumption of isotropic properties in the aquifer. However, in practical engineering, aquifers are often anisotropic, and the influence of this anisotropy on seepage should be considered. Additionally, different projects are located in different geographical areas, resulting in variations in geological conditions and aquifer parameters. Therefore, the aquifer thickness should also be considered as a factor affecting the effectiveness of waterproof curtains. In addition, the actual filter pipe lengths differ from the numerically modeled filter pipe lengths in the standard conditions, depending on the precipitation requirements of a specific project. To make the b_i - s_i curve more applicable to actual geological and construction situations, numerical models are established under different scenarios to simulate and adjust Equation (5). The fitted curve under standard conditions from Figure 5b is chosen as the baseline, and the numerical simulations were used to quantify the impact of permeability anisotropy (k_i), aquifer thickness (M_i), and well screen length (l_i) on the blocking effect of the waterproof curtain.

4.1. Anisotropy of Permeability

The hydraulic permeability of soil exhibits anisotropy due to factors such as depositional history, initial non-uniform consolidation, and variations in stress, resulting in varying characteristics of groundwater flow within the aquifer [44]. The anisotropy ratio of permeability in horizontal and vertical directions, denoted as k_i ($k_i = k_h/k_v$), defines the anisotropy of the aquifer. The vertical flow resistance within the soil becomes more prominent as the anisotropy of hydraulic conductivity increases, and the installation of the curtain exacerbates this effect by inducing vertical flow. The curtain serves to weaken the hydraulic connection between the interior and exterior of the foundation pit, enhancing dewatering efficiency. As the anisotropy of soil permeability increases, the vertical flow velocity decreases, and the blocking effect of the curtain results in the consumption of a greater amount of gravitational potential energy. Keeping all other coefficients constant, only adjusting the k_i parameter, the impact of non-standard permeability anisotropy on the b_i - s_i curve is computed, and the simulation results are presented in Figure 6.

Figure 6 indicates that as the k_i value increases, the b_i - s_i curve does not coincide with the standard curve, providing evidence that k_i does have an impact on the blocking effect of the curtain. The value of k_i varies from 3 to 9, and with increasing values of k_i , the curve deviation becomes more pronounced. The ratio of the numerical solution for the drawdown to the analytical solution increases, suggesting that the permeability anisotropy enhances the blocking effect of the waterproof curtain. To extend Equation (5) to different forms of permeability anisotropy, a correction coefficient function denoted as α is introduced. Its expression is given in Equation (6):

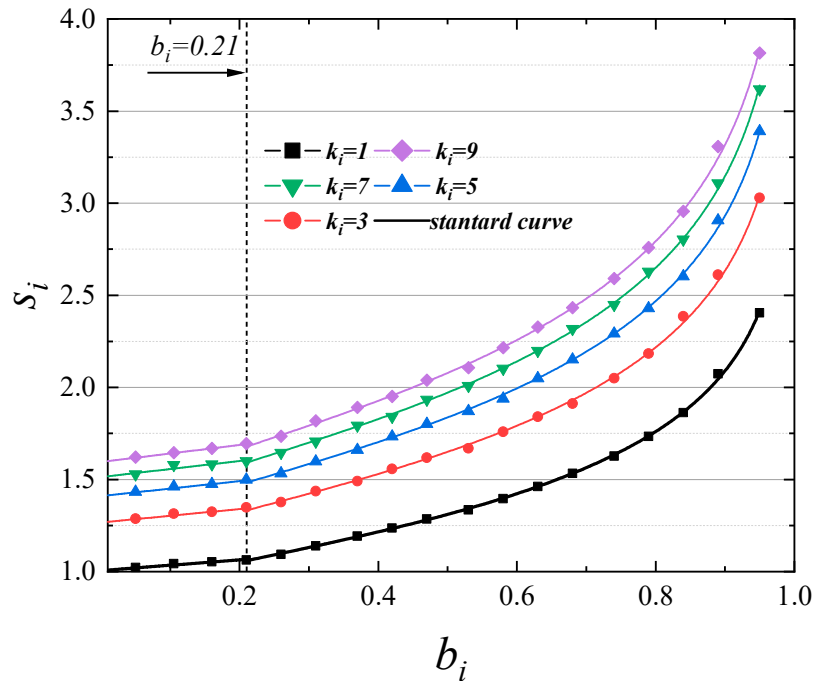


Figure 6. Permeability anisotropy coefficient.

$$\alpha = \left(\frac{k_h}{k_v}\right)^{\frac{1}{5}} \tag{6}$$

4.2. Thickness of the Aquifer

While maintaining the ratio of the insertion depth of the waterproof curtain (b_i) constant, a reduction in the thickness of the aquifer (H) leads to lower piezometric head values in the surrounding area. This results in a decrease in the seepage field area and the vertical hydraulic recharge, ultimately reducing the required dewatering discharge to control drawdown. Changes in the thickness of the aquifer also affect the seepage field distribution, leading to a nonlinear relationship between drawdown and aquifer thickness. Introducing the non-standard aquifer thickness coefficient, by adjusting H_i ($H_i = H/38$), the impact of non-standard aquifer thickness can be calculated on the b_i - s_i curve, as illustrated in Figure 7.

Figure 7 illustrates that the blocking effect curve exhibits varying vertical displacements with changes in H_i , and the linear patterns remain similar across different H_i values. The thickness of the aquifer significantly influences the blocking effect of the curtain. When $H_i > 1$, which indicates an increase in aquifer thickness, the curve tends to shift vertically upwards, indicating enhanced curtain barrier effectiveness. Conversely, when $H_i < 1$, the barrier effect weakens. Similar to the method used for solving permeability anisotropy coefficient, a non-standard aquifer thickness coefficient is determined and represented as β :

$$\beta = H_i^{-0.284 \ln H_i + 0.569} \tag{7}$$

4.3. Pumping Well Screen Length

The pumping capacity of well screens is continuous, and a smaller proportion of well screen length results in longer drainage paths [45]. Under constant discharge conditions, shorter pumping well screen lengths have a more pronounced impact on drawdown levels, leading to greater drawdown depths within the excavation. Therefore, while meeting the fundamental dewatering requirements, it is advisable to select shorter well screen lengths to enhance dewatering efficiency. By adjusting the non-standard well screen length

coefficient, l_i ($l_i = l/H_{ii}$), the impact of non-standard well screen lengths on the b_i - s_i curve can be computed, as illustrated in Figure 8.

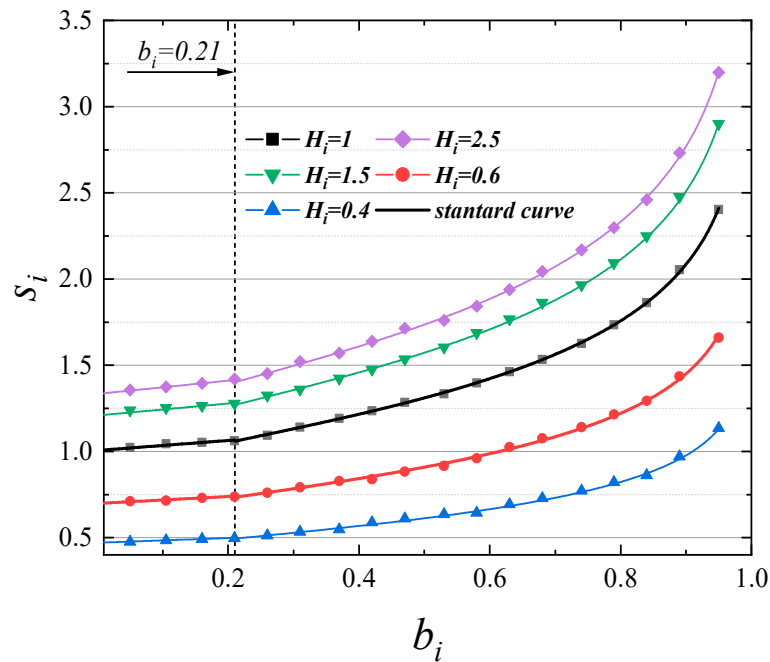


Figure 7. Aquifer thickness coefficient.

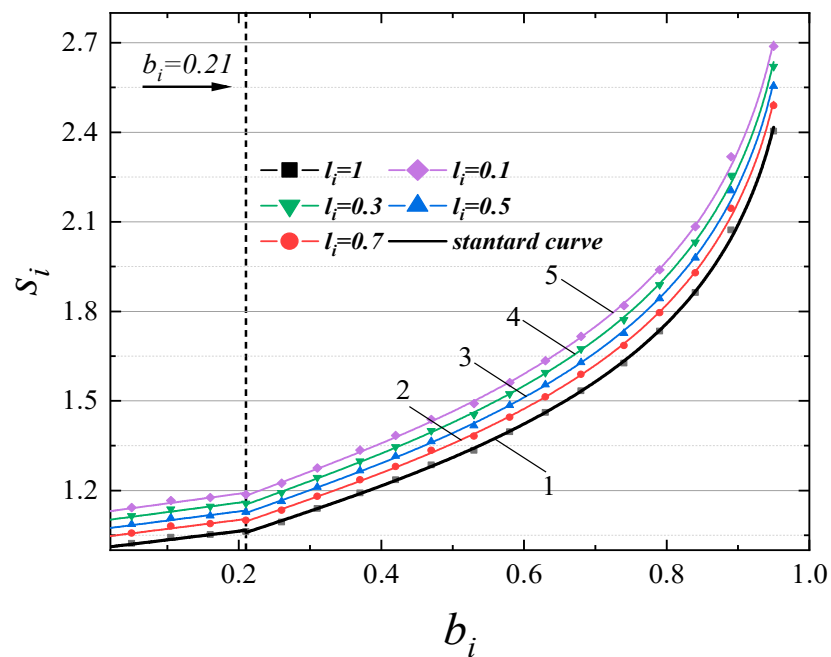


Figure 8. Screen length coefficient.

Figure 8 demonstrates that the blocking effect of the curtain varies with different values of l_i . While the shape of the b_i - s_i curve remains consistent across different l_i values, a reduction in the length of the well screen leads to a vertical upward shift in the curve. This shift provides evidence that the well screen length enhances the blocking effect. Similar to

the method used for solving aquifer thickness coefficient, a coefficient of variation, γ , for non-standard well screen lengths is determined, and its expression is as follows:

$$\gamma = 1.133 \left(\frac{22}{25} \right)^{l_i} \quad (8)$$

4.4. Drawdown Prediction with Suspended Waterproof Curtain

Based on the equivalent well assumption, modifications to the standard curve can be made using variation functions under non-standard conditions. Considering the impact of a single variable on the barrier effect of the curtain, the normalized b_i - s_i curve can be adjusted to a reasonable range. Simultaneously, there are coupling effects among the parameters, leading to a nonlinear increase in s_i . By extending the range of applicability of the b_i - s_i curve using the variation functions derived above, predictions of dewatering drawdown are brought into alignment with actual observations. This yields non-standard characteristic curves for the phreatic aquifer and curtain impact coefficient, denoted as s_{ni} , as expressed below:

$$s_{ni} = s_i \alpha \beta \gamma \quad (9)$$

Combined with the Theis formula, the prediction formula for the dewatering drawdown depth s_d of the phreatic aquifer foundation pit under the action of the waterproof curtain in a soft soil area is derived, and its expression is

$$s_d = s_t s_{ni} \quad (10)$$

5. Application to Field Case

5.1. Project Description

In order to verify the applicability of the calculation method of drawdown depth in the pit under the action of the suspended waterproof curtain proposed above, a large-scale foundation pit required for the construction of a building in Zhuhai City is used as a field case for verification. The layout of this large pit is shown in Figure 9a. The project site is located in a land area with flat terrain and relatively open surroundings. Within 50 m on the north side of the site is a residential community with some elevated buildings, surrounded by grassland and accessed by major urban roads. The absolute elevation of the outdoor ground is 5.35 m.

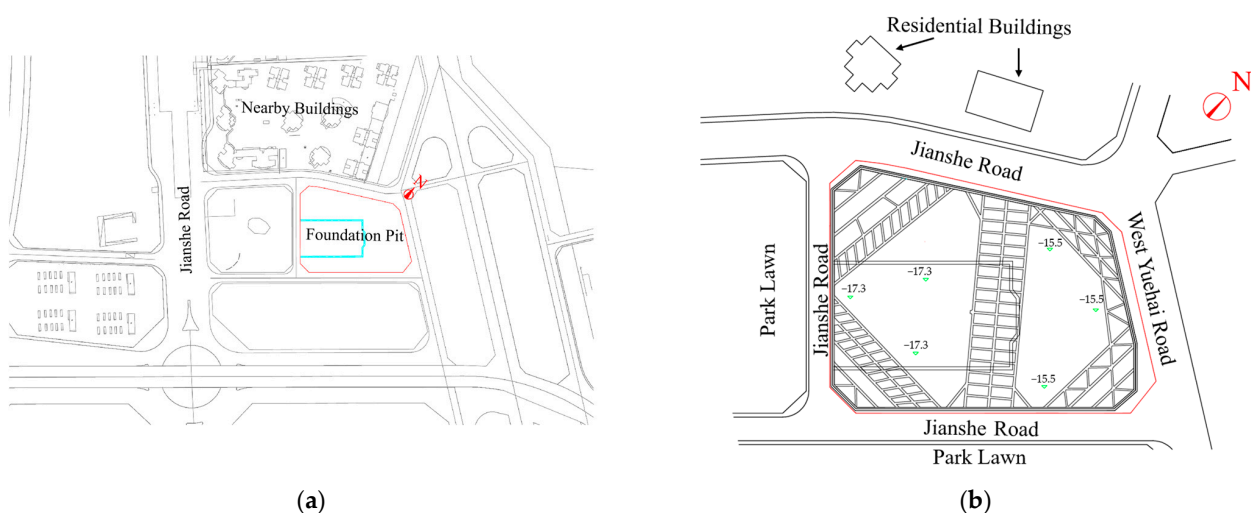


Figure 9. The layout of foundation pit. (a) Environment around the pit. (b) Plan view of the foundation pit.

The pit as a whole is an irregular rectangle which oriented northeast-southwest, with a support perimeter of 368 m and an area of about 8920.6 m². As shown in Figure 9b, the pit

can be divided into two parts: deep pit and shallow pit. The maximum excavation depth of the southwest deep pit is -17.3 m, and the maximum excavation depth of the northeast shallow pit is -15.5 m. The pit adopts a plain concrete wall as a soil and water-retaining structure, with a curtain thickness of 1 m. The length of curtain embedment into the aquifer is 31.3 m for the deep pit and 26.5 m for the shallow pit.

5.2. Hydrogeological Conditions of the Area

The soil profile and soil properties are shown in Figure 10. The soil layers, from top to bottom, are backfill (1_1), silty clay (1_2), coarse sand (1_3), sandy clay (1_4), fine, chalky sand (1_5), chalky clay (2_1), fully weathered granite (3_1), sandy, gravelly soil (4_1), and strongly weathered granite (5_1). The project includes a phreatic aquifer (Aq01), two confined aquifers (Aq I and Aq II), and an aquitard (Ad I and Ad II).

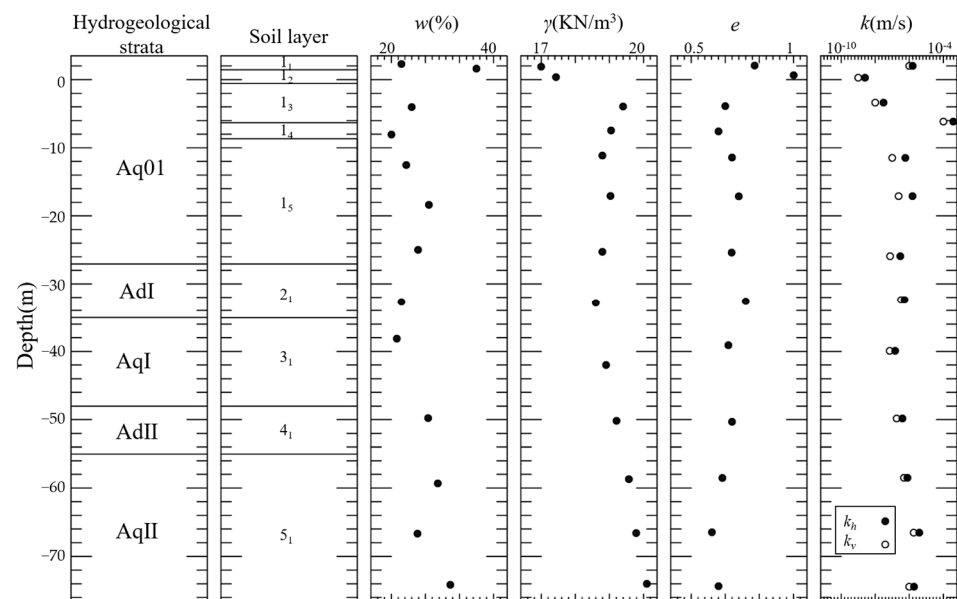


Figure 10. Illustration of geotechnical profile and soil hydraulic conductivity. Note: ω = water content, γ = unit weight, e = void ratio, k_h = horizontal permeability coefficient, and k_v = vertical permeability coefficient.

Detailed information on the aquifer is as follows: During the investigation, groundwater is encountered in all boreholes. As the thickness of the pressurized water in the coarse sand layer (1_3) is thin and its distribution is discontinuous, all of which have an insignificant impact on the construction of the project, it has been determined that the groundwater is submerged at the proposed site. The initial groundwater level of Aq01 is at a depth of 2.33–3.92 m and the source of groundwater is mainly from the upper phreatic aquifer. It is closely connected to atmospheric precipitation and surface water. As a result of the climate and seasons, the water level of the groundwater fluctuates, and when water is abundant, the water level rises. The confined aquifers AqI and AqII are rock fissures filled with pressurized water. It exhibits the following characteristics: it is slightly pressurized, and the distribution of groundwater is greatly affected by the development of fissures in the endowed rock body, with obvious anisotropic characteristics, and it is a non-homogeneous seepage field. In the section where the nodal fissures are more developed, fissure water is more abundant.

The distribution of pumping wells in this project is divided into two parts with 1-1 section, numbered $DW_{1-n(n=1-15)}$ and $DW_{2-n(n=1-12)}$. The length of the pumping wells is 23.0–24.8 m, the effective length of the filter pipe is 5–12 m, and the spacing of the precipitation wells is about 14.8–17.5 m. At the same time, the observation wells are set up around the pumping wells. The location of the pumping wells and the observation wells is shown in Figure 11.

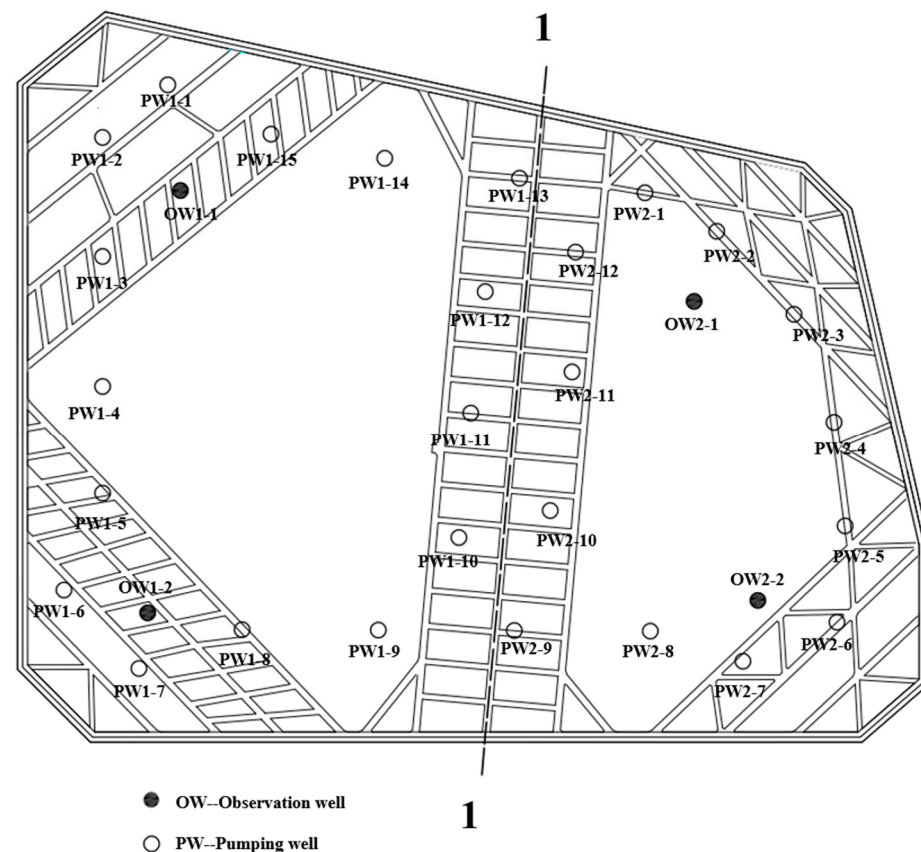


Figure 11. Location of the wells.

5.3. Results

In order to ensure the effect of dewatering, the aquifer needs to be generalized at the design stage. Prior to curtain construction, indoor core tests and field pumping tests are carried out to determine the horizontal and vertical permeability coefficients of the aquifer. These coefficients are 6.322 m/d and 4.33 m/d, respectively.

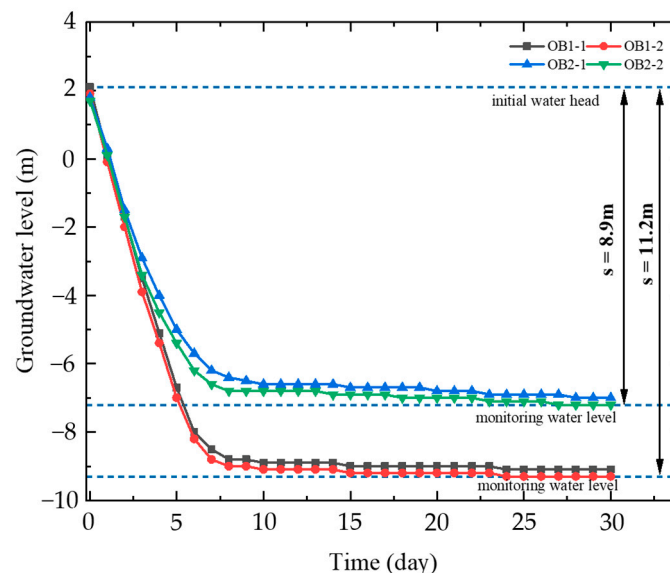
Firstly, from Equations (1) and (4), the equivalent well radii of deep and shallow pits are 41.69 m and 34.3 m, respectively. The total pumping volume of deep and shallow pits are 2400 m³/d and 2000 m³/d, respectively. The depth of pit reduction under the action of pumping wells without waterproof curtains of deep and shallow pits are 3.77 m and 3.76 m. When the curtain is not taken into account, the depth of groundwater reduction generated by the pumping wells can obviously not meet the demand for pit dewatering. The origin method is unable to accurately predict the actual drawdown of groundwater level in the pit. Blindly increasing the pumping volume will cause unnecessary wastage of water resources. The prediction method described in this paper is based on the simulation of an equivalent circular pit model, which proves that the change in the water level in the pit by the precipitation project is independent of the converging shape of the pit according to the results of the study by Lyu et al. [46]. Therefore, according to Equations (5)–(9), the actual parameters of the project are brought in to calculate the curtain-blocking effect coefficients and the value of the variation function. The calculation results are shown in Table 2.

Table 2. Values of the variation function.

Value	Southwest Deep Pit	Northeast Shallow Pit
b_i	0.92	0.88
K_i	1.46	1.46
H_i	0.895	0.79
l_i	0.192	0.226
α	1.077	1.077
β	0.935	0.861
γ	1.106	1.100
S_i	2.191	1.999
S_{ni}	2.44	2.033

Combined with the field observing data, the predicted calculation method case proposed in this paper is verified. The data show that when the total pumping volume of the deep pit on the southwest side and the shallow pit on the northeast side reaches $2400 \text{ m}^3/\text{d}$ and $2000 \text{ m}^3/\text{d}$, respectively, the predicted values of groundwater drawdown in the deep and shallow pits in 30 days are 9.2 m and 7.7 m after the correction coefficients of Table 2 are taken into account, and all of them satisfy the project's safe groundwater drawdown requirements [47].

The pumping capacity of the pumping wells $DW_{1-n(n=1,2,3,5,6,7)}$ on the southwest side and $DW_{2-n(n=1,2,3,6,7,8)}$ on the northeast side of the pit are used as reference, with the pumping capacities of the reference pumping wells on the southwest side ranging from 150 to $165 \text{ m}^3/\text{d}$, and the pumping capacities of the pumping wells on the northeast side ranging from 160 to $168 \text{ m}^3/\text{d}$. At the same time, based on the observation data from the observation wells (OW_{1-1} , OW_{1-2} , OW_{2-1} , and OW_{2-2}), the groundwater level changes in the pit are reflected. When the fluctuation of water level in the observation wells is less than $2\text{--}3 \text{ m}$, it is considered to reach a stable groundwater level [48]. The observation process is accumulated for 30 days. Figure 12 shows the groundwater level observation data in the observation wells.

**Figure 12.** Variation of groundwater of observation wells.

As the working time of the pumping well grows, the groundwater level in the pit decreases in depth. The change in drawdown decreases is first steep and then becomes flat. The groundwater level between the two observation wells in the deep and shallow pits is basically the same, indicating that the water pressure in the pits is uniformly distributed in the process of precipitation, and the maximum depth of the groundwater level in the

deep and shallow pits after the final stabilization is -11.2 m and -8.9 m. Accordingly, the study concludes that the predicted value of groundwater drawdown in the pits has a safe redundancy with a value of between 16 and 21%.

Since the waterproof curtain did not completely isolate the hydraulic connection between the inside and outside of the pit, the operation of the pumping wells in the pit has a certain impact on the groundwater outside the pit. The groundwater outside the pit fluctuates, but the head change value is between 1.0 and 1.5 m, which meets the demand for groundwater control outside the pit. As the project is in a coastal area with a strong recharge capacity of the aquifer, the head outside the pit can recover to the initial state similar to the pre-construction state. The foundation pit surface remains stable throughout the excavation and dewatering process, which indicates that the calculation method for predicting the amount of groundwater drawdown in the pit proposed in this study is feasible.

6. Conclusions

Based on the theory of three-dimensional seepage analysis of phreatic aquifer, a formula is proposed to predict the groundwater drawdown in the foundation pit under the action of the suspended waterproof curtain and pumping wells. The formula is applied to the field foundation pit dewatering project. The comparison of the observed and calculated values shows that the prediction and calculation method is reasonable and the algorithm is simple. In the actual project, the depth of curtain embedding and pumping volume can be determined to determine the depth of groundwater drawdown in the pit. Thus, this calculation method provides a reference for predicting the depth of groundwater drawdown in the pit. Based on the results of this study, the following conclusions are drawn:

1. The waterproof curtain can improve the efficiency of pit dewatering by changing the seepage field distribution and thus reducing the hydraulic connection between the inside and outside of the pit. The Thies formula does not take into account the influence of the change in the flow field morphology on the groundwater seepage, and the influence coefficient must be introduced to correct the calculation results.
2. Based on the equivalent well theory, solve the characteristic curve of curtain ratio (b_i) and drawdown ratio (s_i) under each influence coefficient. Quantify the curve to get the curtain-blocking effect coefficient under the normalized state. Considering the coupling effect generated by k_i , M_i , l_i , and the waterproof curtain, the finite difference method is adopted, and the non-standard variability function is obtained by regression analysis of numerical results. The non-standard variability function reflects the coupled influence of the curtain barrier effect and project parameters on the amount of groundwater drawdown in the pit.
3. This paper presents a calculation method for predicting the amount of groundwater drawdown in a pit for a certain amount of pumping. The established equation is applied to the Zhuhai field pit pumping design. The predicted value is close to the field wells observing results, and the original design scheme maintains a 16–21% safe margin. In addition, the change of groundwater drawdown outside the pit is less than 1.5 m, which ensures the environment inside and outside the excavation pit is safe. The prediction method is reasonable.

Author Contributions: Conceptualization, J.S.; methodology, J.S.; software, Y.C.; validation, Y.C.; formal analysis, Y.C.; investigation, Z.Y.; resources, Z.Y.; data curation, Y.C.; writing—original draft preparation, Y.C.; writing—review and editing, J.S. and D.L.; visualization, Y.C.; supervision, J.S. and D.L.; project administration, J.S.; funding acquisition, J.S. All authors have read and agreed to the published version of the manuscript.

Funding: This study was funded by the Natural Science Foundation of China, grant number 51708188.

Data Availability Statement: Data are contained within the article.

Conflicts of Interest: The authors declare no conflicts of interest.

References

1. Cao, Y.; Zhang, R.; Zhang, D.; Zhou, C. Urban Agglomerations in China: Characteristics and Influencing Factors of Population Agglomeration. *Chin. Geogr. Sci.* **2023**, *33*, 719–735. [[CrossRef](#)]
2. Wang, Y.; Jiao, J.J.; Cherry, J.A.; Lee, C.M. Contribution of the aquitard to the regional groundwater hydrochemistry of the underlying confined aquifer in the Pearl River Delta, China. *Sci. Total Environ.* **2013**, *461*, 663–671. [[CrossRef](#)] [[PubMed](#)]
3. Xu, Y.-S.; Shen, S.-L.; Du, Y.-J. Geological and hydrogeological environment in Shanghai with geohazards to construction and maintenance of infrastructures. *Eng. Geol.* **2009**, *109*, 241–254. [[CrossRef](#)]
4. Xu, Y.-S.; Wu, H.-N.; Shen, J.S.; Zhang, N. Risk and impacts on the environment of free-phase biogas in quaternary deposits along the Coastal Region of Shanghai. *Ocean Eng.* **2017**, *137*, 129–137. [[CrossRef](#)]
5. Zhang, X.; Yang, J.; Zhang, Y.; Gao, Y. Cause investigation of damages in existing building adjacent to foundation pit in construction. *Eng. Fail. Anal.* **2018**, *83*, 117–124. [[CrossRef](#)]
6. Wan, X.; Ding, J.; Jiao, N.; Sun, S.; Liu, J.; Guo, Q. Observed Performance of Long-Zoned Excavation with Suspended Waterproof Curtain in Yangtze River Floodplain. *J. Perform. Constr. Facil.* **2022**, *36*, 04022018. [[CrossRef](#)]
7. Wang, Y.; Jiao, J.J. Origin of groundwater salinity and hydrogeochemical processes in the confined Quaternary aquifer of the Pearl River Delta, China. *J. Hydrol.* **2012**, *438*, 112–124. [[CrossRef](#)]
8. Huang, Y.; Bao, Y.; Wang, Y. Analysis of geo-environmental hazards in urban underground space development in Shanghai. *Nat. Hazards* **2015**, *75*, 2067–2079. [[CrossRef](#)]
9. Wang, J.X.; Deng, Y.S.; Wang, X.B.; Liu, X.T.; Zhou, N.Q. Numerical evaluation of a 70-m deep hydropower station foundation pit de-watering. *Environ. Earth Sci.* **2022**, *81*, 364. [[CrossRef](#)]
10. Sun, Z.; Li, H.; Bao, Y.; Meng, X.; Zhang, D. Intelligent Risk Prognosis and Control of Foundation Pit Excavation Based on Digital Twin. *Buildings* **2023**, *13*, 247. [[CrossRef](#)]
11. Cao, C.; Shi, C.; Liu, L.; Liu, J. Evaluation of the effectiveness of an alternative to control groundwater inflow during a deep excavation into confined aquifers. *Environ. Earth Sci.* **2020**, *79*, 502. [[CrossRef](#)]
12. Barbu, C.; Sabău, A.-D.; Manoli, D.-M.; Șerbulea, M.-S.; Erbașu, R.; Tăpuși, D.; Szlachetka, O.; Dziecioł, J.; Baryła, A.; Dohojda, M.; et al. Analysis of the Water/Cement/Bentonite Ratio Used for Construction of Cut-Off Walls. *Buildings* **2023**, *13*, 2922. [[CrossRef](#)]
13. Mahmoudpour, M.; Khomehchiyan, M.; Nikudel, M.R.; Ghassemi, M.R. Numerical simulation and prediction of regional land sub-sidence caused by groundwater exploitation in the southwest plain of Tehran, Iran. *Eng. Geol.* **2016**, *201*, 6–28. [[CrossRef](#)]
14. Xu, Y.-S.; Wu, H.-N.; Wang, B.Z.-F.; Yang, T.-L. Dewatering induced subsidence during excavation in a Shanghai soft deposit. *Environ. Earth Sci.* **2017**, *76*, 351. [[CrossRef](#)]
15. Chen, J.J.; Zhang, L.Y.; Zhang, J.F.; Zhu, Y.F.; Wang, J.H. Field Tests, Modification, and Application of Deep Soil Mixing Method in Soft Clay. *J. Geotech. Geo-Environ. Eng.* **2013**, *139*, 24–34. [[CrossRef](#)]
16. Xu, Y.-S.; Shen, S.-L.; Ma, L.; Sun, W.-J.; Yin, Z.-Y. Evaluation of the blocking effect of retaining walls on groundwater seepage in aquifers with different insertion depths. *Eng. Geol.* **2014**, *183*, 254–264. [[CrossRef](#)]
17. Wang, Z.-F.; Shen, S.-L.; Ho, C.-E.; Kim, Y.-H. Investigation of field-installation effects of horizontal twin-jet grouting in Shanghai soft soil deposits. *Can. Geotech. J.* **2013**, *50*, 288–297. [[CrossRef](#)]
18. Du, S.; Liu, P.; Wang, W.; Shi, W.; Li, Q.; Li, J.; Li, J. Numerical Simulation and Analysis of the Influencing Factors of Foundation Pit Dewatering under a Coupled Radial Well and Curtain. *Water* **2023**, *15*, 1839. [[CrossRef](#)]
19. Zeng, C.-F.; Zheng, G.; Xue, X.-L.; Mei, G.-X. Combined recharge: A method to prevent ground settlement induced by redevelopment of recharge wells. *J. Hydrol.* **2019**, *568*, 1–11. [[CrossRef](#)]
20. Zeng, C.-F.; Xue, X.-L.; Zheng, G.; Xue, T.-Y.; Mei, G.-X. Responses of retaining wall and surrounding ground to pre-excavation dewatering in an alternated multi-aquifer-aquitard system. *J. Hydrol.* **2018**, *559*, 609–626. [[CrossRef](#)]
21. Pujades, E.; Jurado, A.; Carrera, J.; Vazquez-Sune, E.; Dassargues, A. Hydrogeological assessment of non-linear underground en-closures. *Eng. Geol.* **2016**, *207*, 91–102. [[CrossRef](#)]
22. Sundell, J.; Rosén, L.; Norberg, T.; Haaf, E. A probabilistic approach to soil layer and bedrock-level modeling for risk assessment of groundwater drawdown induced land subsidence. *Eng. Geol.* **2016**, *203*, 126–139. [[CrossRef](#)]
23. Zhang, X.; Hu, M.; Chen, X.; Dong, J.; Liu, S. Research on Subsidence Induced by the Dewatering–Curtain Interaction in the Deep Foundation Pit of the Shield Launching Shaft in Shenzhen, China. *Water* **2023**, *15*, 1798. [[CrossRef](#)]
24. Wang, J.; Wu, Y.; Liu, X.; Yang, T.; Wang, H.; Zhu, Y. Areal subsidence under pumping well–curtain interaction in subway foundation pit dewatering: Conceptual model and numerical simulations. *Environ. Earth Sci.* **2016**, *75*, 198. [[CrossRef](#)]
25. You, Y.; Yan, C.; Xu, B.; Liu, S.; Che, C. Optimization of dewatering schemes for a deep foundation pit near the Yangtze River, China. *J. Rock Mech. Geotech. Eng.* **2018**, *10*, 555–566. [[CrossRef](#)]
26. Chen, Z.; Huang, J.; Zhan, H.; Wang, J.; Dou, Z.; Zhang, C.; Chen, C.; Fu, Y. Optimization schemes for deep foundation pit dewatering under complicated hydrogeological conditions using MODFLOW-USG. *Eng. Geol.* **2022**, *303*, 106653. [[CrossRef](#)]
27. Wu, Y.-X.; Shen, S.-L.; Yuan, D.-J. Characteristics of dewatering induced drawdown curve under blocking effect of retaining wall in aquifer. *J. Hydrol.* **2016**, *539*, 554–566. [[CrossRef](#)]
28. Wang, X.-W.; Xu, Y.-S. Impact of the Depth of Diaphragm Wall on the Groundwater Drawdown during Foundation Dewatering Considering Anisotropic Permeability of Aquifer. *Water* **2021**, *13*, 418. [[CrossRef](#)]

29. Yang, T.; Tong, L.Y.; El Naggar, M.H.; Yan, X. Hydraulic head difference at two sides of suspended waterproof curtain during mul-ti-grade dewatering of excavation. *Undergr. Space* **2023**, *10*, 137–149. [[CrossRef](#)]
30. Wu, Y.-X.; Shen, S.-L.; Wu, H.-N.; Xu, Y.-S.; Yin, Z.-Y.; Sun, W.-J. Environmental protection using dewatering technology in a deep confined aquifer beneath a shallow aquifer. *Eng. Geol.* **2015**, *196*, 59–70. [[CrossRef](#)]
31. Wang, J.; Liu, X.; Wu, Y.; Liu, S.; Wu, L.; Lou, R.; Lu, J.; Yin, Y. Field experiment and numerical simulation of coupling non-Darcy flow caused by curtain and pumping well in foundation pit dewatering. *J. Hydrol.* **2017**, *549*, 277–293. [[CrossRef](#)]
32. Wang, J.; Liu, X.; Liu, S.; Zhu, Y.; Pan, W.; Zhou, J. Physical model test of transparent soil on coupling effect of cut-off wall and pumping wells during foundation pit dewatering. *Acta Geotech.* **2019**, *14*, 141–162. [[CrossRef](#)]
33. Wang, X.-W.; Yang, T.-L.; Xu, Y.-S.; Shen, S.-L. Evaluation of optimized depth of waterproof curtain to mitigate negative impacts during dewatering. *J. Hydrol.* **2019**, *577*, 123969. [[CrossRef](#)]
34. Shen, S.-L.; Wu, Y.-X.; Misra, A. Calculation of head difference at two sides of a cut-off barrier during excavation dewatering. *Comput. Geotech.* **2017**, *91*, 192–202. [[CrossRef](#)]
35. Zhang, X.; Wang, X.; Xu, Y. Influence of Filter Tube of Pumping Well on Groundwater Drawdown during Deep Foundation Pit Dewatering. *Water* **2021**, *13*, 3297. [[CrossRef](#)]
36. Vilarrasa, V.; Carrera, J.; Jurado, A.; Pujades, E.; Vázquez-Suné, E. A methodology for characterizing the hydraulic effectiveness of an annular low-permeability barrier. *Eng. Geol.* **2011**, *120*, 68–80. [[CrossRef](#)]
37. Pujades, E.; López, A.; Carrera, J.; Vázquez-Suné, E.; Jurado, A. Barrier effect of underground structures on aquifers. *Eng. Geol.* **2012**, *145*, 41–49. [[CrossRef](#)]
38. Bear, J. *Hydraulics of Groundwater*; McGraw-Hill: New York, NY, USA, 2012.
39. Xue, Y.Q.; Wu, J.C. *Groundwater Dynamics*; Geological Publish House: Beijing, China, 2010; pp. 20–96. (In Chinese)
40. Theis, C.V. The relation between the lowering of the Piezometric surface and the rate and duration of discharge of a well using ground-water storage. *Trans. Am. Geophys. Union* **1935**, *16*, 519–524. [[CrossRef](#)]
41. Lancia, M.; Su, H.; Tian, Y.; Xu, J.; Andrews, C.; Lerner, D.N.; Zheng, C. Hydrogeology of the Pearl River Delta, southern China. *J. Maps* **2020**, *16*, 388–395. [[CrossRef](#)]
42. Chen, C.X.; Lin, M. *Groundwater Dynamics*; China University of Geosciences Press: Wuhan, China, 1999; pp. 59–69. (In Chinese)
43. Shen, S.L.; Wu, Y.X.; Xu, Y.S.; Hino, T.; Wu, H.N. Evaluation of hydraulic parameters from pumping tests in multi-aquifers with vertical leakage in Tianjin. *Comput. Geotech.* **2015**, *68*, 196–207. [[CrossRef](#)]
44. Yao, M.; Wang, H.; Yu, Q.; Li, H.; Xia, W.; Wang, Q.; Huang, X.; Lin, J. Anisotropy Study on the Process of Soil Permeability and Consolidation in Reclamation Areas: A Case Study of Chongming East Shoal in Shanghai. *Buildings* **2023**, *13*, 3059. [[CrossRef](#)]
45. Xu, Y.S.; Yan, X.X.; Shen, S.L.; Zhou, A.N. Experimental investigation on the blocking of groundwater seepage from a waterproof curtain during pumped dewatering in an excavation. *Hydrogeol. J.* **2019**, *27*, 2659–2672. [[CrossRef](#)]
46. Lyu, H.-M.; Shen, S.-L.; Wu, Y.-X.; Zhou, A.-N. Calculation of groundwater head distribution with a close barrier during excavation dewatering in confined aquifer. *Geosci. Front.* **2021**, *12*, 791–803. [[CrossRef](#)]
47. Wang, J.; Feng, B.; Guo, T.; Wu, L.; Lou, R.; Zhou, Z. Using partial penetrating wells and curtains to lower the water level of confined aquifer of gravel. *Eng. Geol.* **2013**, *161*, 16–25. [[CrossRef](#)]
48. Yao, T.Q. *Manual of Pit Descending*; China Construction Industry Press: Beijing, China, 2006.

Disclaimer/Publisher’s Note: The statements, opinions and data contained in all publications are solely those of the individual author(s) and contributor(s) and not of MDPI and/or the editor(s). MDPI and/or the editor(s) disclaim responsibility for any injury to people or property resulting from any ideas, methods, instructions or products referred to in the content.